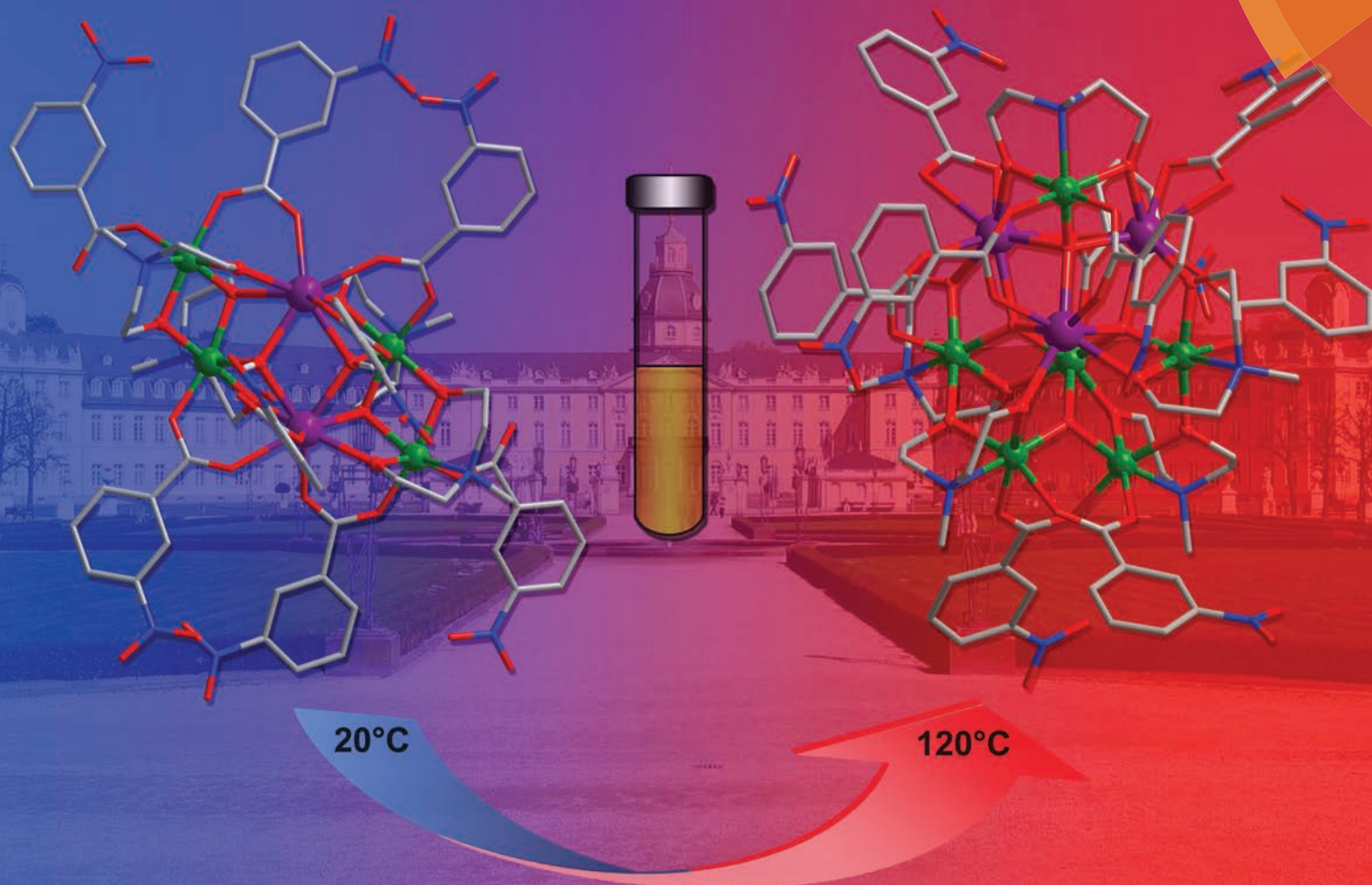


Dalton Transactions

An international journal of inorganic chemistry
www.rsc.org/dalton



ISSN 1477-9226



PAPER

Valeriu Mereacre, Annie K. Powell *et al.*

A single molecule magnet to single molecule magnet transformation via a solvothermal process: $\text{Fe}_4\text{Dy}_2 \rightarrow \text{Fe}_6\text{Dy}_3$

175 YEARS

Cite this: *Dalton Trans.*, 2016, **45**, 98

A single molecule magnet to single molecule magnet transformation *via* a solvothermal process: $\text{Fe}_4\text{Dy}_2 \rightarrow \text{Fe}_6\text{Dy}_3^\dagger$

Sihuai Chen,^a Valeriu Mereacre,^{*a} Christopher E. Anson^a and Annie K. Powell^{*a,b}

Two series of heterometallic $\text{Fe}^{\text{III}}\text{-Ln}^{\text{III}}$ compounds, $[\text{Fe}_4\text{Ln}_2(\mu_3\text{-OH})_2(\text{mdea})_4(m\text{-NO}_2\text{C}_6\text{H}_4\text{COO})_8]\cdot 3\text{MeCN}$ where Ln = Y (**1**) and Dy (**2**) and $[\text{Fe}_6\text{Ln}_3(\mu_4\text{-O})_3(\mu_3\text{-O})(\text{mdea})_5(m\text{-NO}_2\text{C}_6\text{H}_4\text{COO})_9]\cdot 3\text{MeCN}$ where Ln = Y (**3**) and Dy (**4**), were synthesized. Compounds **1** and **2** were obtained under ambient conditions, whereas **3** and **4** were obtained *via* a solvothermal transformation process by heating **1** or **2** at 120 °C in MeCN. The magnetic properties of all four compounds have been measured and show that compounds **2** and **4** containing Dy^{III} ions exhibit slow relaxation of magnetization characteristic of Single Molecule Magnetic (SMM) behaviour.

Received 6th October 2015,
Accepted 31st October 2015

DOI: 10.1039/c5dt03909f

www.rsc.org/dalton

Introduction

The design, synthesis and investigation of polynuclear coordination clusters have been the focus of intense research activity because of their interesting electronic and magnetic features, which include the observation of single molecule magnetic (SMM) behaviour.¹ Single-molecule magnets (SMMs) are a class of molecular superparamagnetic metal clusters in which a high spin ground state and the negative zero-field splitting of the ground state lead to a slow relaxation of magnetization, with these effects generally being observed at low temperatures where quantum tunnelling of the relaxation becomes blocked.² In the quest for systems showing SMM behaviour with high blocking temperature and slow relaxation times, a large number of 3d–4f polynuclear coordination clusters (CCs) have been studied with the idea that combining the large magnetic anisotropy of lanthanide(III) ions and the high spin-states of many transition metal ions could provide suitable SMMs.^{3,4}

In this search, ligands bearing alkoxy groups, which are capable of both chelating and bridging between metal centres, such as the *N*-substituted diethanolamines, and which are known to lead to polynuclear Fe^{III} and 4f CCs,^{5,6} have been found to be ideal for stabilising 3d–4f CCs⁷ due to the fact that

the hard-donor oxygens are likely to bind to the oxophilic lanthanide ions, leaving the softer donor nitrogen to act as the central tripodal ligand binding the softer transition metal ions and providing the anchor point for the 3d/4f coordination cluster. Thus the deprotonated alcohol arms provide chelating and bridging capabilities and facilitate the formation of high nuclearity 3d–4f CCs.

From a synthetic point of view, CCs are metastable species produced by solvolysis of metal ions and are prevented from reaching the thermodynamic continuous phase end-point through the availability of encapsulating ligand species.^{1b} Whereas ambient conditions have been successfully applied to produce a large variety of CCs, hydro- and solvo-thermal synthesis often leads to coordination polymers and MOFs with continuous rather than finite 0D structures. However, careful control of the conditions has been shown to lead to the production of finite CC systems.^{8a,b} This approach appears to be particularly promising for systems incorporating 4f ions. In this technique high temperatures are applied to the reactions in solvents with low boiling points. The resulting compounds produced under solvothermal conditions may exhibit structural diversity and unique properties.⁹ For example, we recently reported two $\text{Fe}_4^{\text{III}}\text{Dy}_4^{\text{III}}$ clusters obtained *via* a solvothermal treatment of two different $\text{Fe}^{\text{III}}\text{-Dy}^{\text{III}}$ compounds produced from reactions conducted under normal conditions.^{8a}

In this paper, we present the synthesis, structures and magnetic properties of two sets of $\text{Fe}^{\text{III}}\text{-Ln}^{\text{III}}$ compounds formulated as $[\text{Fe}_4\text{Ln}_2(\mu_3\text{-OH})_2(\text{mdea})_4(m\text{-NO}_2\text{C}_6\text{H}_4\text{COO})_8]$ where Ln = Y (**1**) and Dy (**2**) and $[\text{Fe}_6\text{Ln}_3(\mu_4\text{-O})_3(\mu_3\text{-O})(\text{mdea})_5(m\text{-NO}_2\text{C}_6\text{H}_4\text{COO})_9]$ where Ln = Y (**3**) and Dy (**4**), among which compounds **3** and **4** were synthesised *via* a transformation process by heating **1** or **2** in MeCN under solvothermal conditions, respectively.

^aInstitute of Inorganic Chemistry, Karlsruhe Institute of Technology, Engesserstrasse 15, 76131 Karlsruhe, Germany. E-mail: valeriu.mereacre@kit.edu, annie.powell@kit.edu

^bInstitute of Nanotechnology, Karlsruhe Institute of Technology, Hermann-von-Helmholtz Platz 1, 76344 Eggenstein-Leopoldshafen, Germany

†Electronic supplementary information (ESI) available. CCDC 1429780 and 1429781. For ESI and crystallographic data in CIF or other electronic format see DOI: 10.1039/c5dt03909f



Experimental

General procedures

All chemicals and solvents were obtained from commercial sources and were used without further purification. All reactions were carried out under aerobic conditions. $[\text{Fe}_3^{\text{III}}\text{O}(\text{m-NO}_2\text{C}_6\text{H}_4\text{COO})(\text{H}_2\text{O})_3]^+(\text{m-NO}_2\text{C}_6\text{H}_4\text{COO})^-$ was prepared according to a previously reported procedure.¹⁰ Compounds **3** and **4** were synthesised by sealing the reaction mixtures in transparent 10 mL Biotage Microwave Reaction Kits (<http://www.biotage.com>) and placing the vials in an oven at 120 °C under normal solvothermal conditions, rather than under microwave conditions. Elemental analyses for C, H, and N were performed using an Elementar Vario EL analyser and were carried out at the Institute of Inorganic Chemistry, Karlsruhe Institute of Technology. IR spectra were recorded on a Perkin-Elmer Spectrum One spectrometer using KBr pellets.

Synthesis of $[\text{Fe}_4\text{Y}_2(\mu_3\text{-OH})_2(\text{mdea})_4(\text{m-NO}_2\text{C}_6\text{H}_4\text{COO})_8]\cdot 3\text{MeCN}$ (**1**)

A solution of $[\text{Fe}_3\text{O}(\text{m-NO}_2\text{C}_6\text{H}_4\text{COO})_6(\text{H}_2\text{O})_3]^+(\text{m-NO}_2\text{C}_6\text{H}_4\text{COO})^-$ (0.164 g, 0.12 mmol), $\text{Y}(\text{NO}_3)_3\cdot 6\text{H}_2\text{O}$ (0.048 g, 0.13 mmol) and mdeaH_2 (0.121 g, 0.10 mmol) in MeCN (30 ml) was stirred at room temperature for one hour. The clear brown solution was left undisturbed. After one day, yellow crystals were collected, washed with MeCN and dried in air. Yield: 42% (based on Y). Anal. Calc. for $\text{C}_{82}\text{H}_{87}\text{N}_{15}\text{O}_{42}\text{Fe}_4\text{Y}_2$: C, 41.81; H, 3.72; N, 8.92; found C, 41.67; H, 3.74; N, 8.81%. IR (KBr) (cm^{-1}): 2874 (w), 1646 (m), 1617 (m), 1600 (s), 1564 (s), 1531 (s), 1479 (m), 1438 (m), 1396 (vs), 1350 (s), 1328 (m), 1269 (mw), 1158 (mw), 1073 (m), 1023 (w), 999 (mw), 906 (mw), 818 (mw), 788 (m), 762 (w), 724 (s), 653 (mw), 585 (m).

$[\text{Fe}_4\text{Dy}_2(\mu_3\text{-OH})_2(\text{mdea})_4(\text{m-NO}_2\text{C}_6\text{H}_4\text{COO})_8]\cdot 3\text{MeCN}$ (**2**)

This compound was obtained using the same procedure as that for **1**, but using $\text{Dy}(\text{NO}_3)_3\cdot 6\text{H}_2\text{O}$ in place of $\text{Y}(\text{NO}_3)_3\cdot 6\text{H}_2\text{O}$. Yield: 10% (based on Dy). Anal. Calc. for $\text{C}_{76}\text{H}_{78}\text{N}_{12}\text{O}_{42}\text{Fe}_4\text{Dy}_2$ (corresponding to replacement of lattice MeCN by $2\text{H}_2\text{O}$): C, 37.78; H, 3.42; N, 6.96; found C, 37.73; H, 3.24; N, 6.98%. IR (KBr) (cm^{-1}): 3436 (br), 2861 (m), 1616 (s), 1597 (s), 1564 (s), 1531 (s), 1481 (s), 1437 (m), 1396 (vs), 1351 (s), 1270 (m), 1159 (m), 1073 (s), 1023 (m), 1001 (m), 908 (m), 819 (m), 789 (s), 763 (m), 724 (s), 654 (m), 585 (m).

Synthesis of $[\text{Fe}_6\text{Y}_3(\mu_4\text{-O})_3(\mu_3\text{-O})(\text{mdea})_5(\text{m-NO}_2\text{C}_6\text{H}_4\text{COO})_9]\cdot 3\text{MeCN}$ (**3**)

A mixture of **1** (0.020 g, 0.01 mmol) in MeCN (2 mL) was sealed in a 10 mL Biotage Microwave Reaction Kit. The reaction mixture was kept at 120 °C for 72 h. After cooling, the brown crystals were collected, washed with MeCN and dried in air. Yield: 27% (based on Y). Anal. Calc. for $\text{C}_{88}\text{H}_{91}\text{N}_{14}\text{O}_{50}\text{Fe}_6\text{Y}_3$ (loss of lattice MeCN): C, 38.48; H, 3.34; N, 7.14; found C, 38.13; H, 3.20; N, 7.07%. IR (KBr) (cm^{-1}): 3438 (br), 2862 (m), 1612 (s), 1570 (m), 1531 (s), 1480 (m), 1437 (m), 1404 (s), 1351 (s), 1269 (w), 1160 (w), 1102 (m), 1077 (m), 1034 (w), 998 (w), 907 (w), 827 (w), 788 (w), 723 (m), 653 (w), 604 (w), 578 (w).

Synthesis of $[\text{Fe}_6\text{Dy}_3(\mu_4\text{-O})_3(\mu_3\text{-O})(\text{mdea})_5(\text{m-NO}_2\text{C}_6\text{H}_4\text{COO})_9]\cdot 3\text{MeCN}$ (**4**)

This compound was obtained using the same procedure as that for **3**, but using **2** in place of **1**. Yield: 36% (based on Dy). Anal. Calc. for $\text{C}_{94}\text{H}_{100}\text{N}_{17}\text{O}_{50}\text{Fe}_6\text{Dy}_3$: C, 36.53; H, 3.26; N, 7.70; found C, 36.46; H, 3.23; N, 7.52%. IR (KBr) (cm^{-1}): 3430 (br), 3084 (w), 2863 (m), 1612 (s), 1570 (m), 1532 (s), 1481 (m), 1438 (m), 1405 (s), 1351 (s), 1270 (w), 1160 (w), 1102 (m), 1076 (m), 1034 (w), 997 (w), 907 (w), 826 (w), 788 (w), 724 (m), 653 (w), 604 (w), 579 (w).

Physical measurements

X-Ray crystallography. Data for **1** were collected at the SCD beamline of the ANKA synchrotron, Karlsruhe, Germany, on a Bruker SMART Apex diffractometer using Si-monochromated radiation of wavelength 0.80000 Å. Data for **4** were collected on a Stoe IPDS II diffractometer using graphite-monochromated Mo-K α radiation. Semi-empirical absorption corrections were applied. The structures were solved using direct methods, followed by a full-matrix least-squares refinement against F^2 (all data) using SHELXL-2014.¹¹ Anisotropic refinement was used for all ordered non-hydrogen atoms. All hydrogen atoms were placed in calculated positions using a riding model. Disorder in the nitrobenzoate ligands was modelled using sets of isotropic atoms of 50% occupancy. Geometrical restraints (SADI) and constraints (AFIX 66) were applied as necessary. Crystallographic and structure refinement data are summarised in Table 1.

Crystallographic data (excluding structure factors) for the structures in this paper have been deposited with the Cambridge Crystallographic Data Centre as supplementary publication no. CCDC 1429780 and 1429781.

Powder X-ray measurements were made with a Stoe STADI-P diffractometer using Cu-K α radiation.

Magnetic measurements. The magnetic susceptibility measurements were collected on a Quantum Design SQUID magnetometer MPMS-XL. This magnetometer works between 1.8 and 300 K for dc applied fields ranging from -7 to 7 T. Measurements were carried out on finely ground polycrystalline samples constrained with eicosane. The dc magnetic susceptibility data for compounds **1-4** were collected in the 1.8-300 K temperature range at 1000 Oe. Ac susceptibility measurements were performed with an oscillating field of 3 Oe and frequencies ranging from 1 to 1500 Hz. The magnetic data were corrected for diamagnetic contributions of the sample holder.

Results and discussion

Synthesis and crystal structures

In order to synthesise structurally diverse Fe^{III} -4f aggregates, an assisted self-assembly approach has been applied often using Fe^{III} carboxylate triangles $[\text{Fe}_3^{\text{III}}\text{O}(\text{RCOO})_6(\text{H}_2\text{O})_3]^+$ as starting material.¹² The topologies of the metastable products are influenced not only by the metal salts used, but also by the reaction conditions (temperature, pressure, acidity and so on),



Table 1 Crystallographic and structure refinement data for compounds 1–4

	1	2	3	4
Formula	C ₈₂ H ₈₇ N ₁₅ O ₄₂ Fe ₄ Y ₂	C ₈₂ H ₈₇ N ₁₅ O ₄₂ Fe ₄ Dy ₂	C ₉₄ H ₁₀₀ N ₁₇ O ₅₀ Fe ₆ Y ₃	C ₉₄ H ₁₀₀ N ₁₇ O ₅₀ Fe ₆ Dy ₃
M _r	2355.88	2505.11	2868.91	3090.50
Crystal system	Monoclinic	Monoclinic	Triclinic	Triclinic
Space group	C2/c	C2/c	Pī	Pī
T (K)	150(2)	150(2)	298(2)	150(2)
a (Å)	31.177(4)	31.1882	13.9126	13.8939(9)
b (Å)	15.660(2)	15.6817	16.8878	16.7523(12)
c (Å)	20.673(3)	20.7311	24.9901	24.8472(16)
α (°)	90	90	81.858	81.772(5)
β (°)	95.539(2)	94.922	83.118	83.121(5)
γ (°)	90	90	86.085	85.507(5)
V (Å ³)	10 046(2)	10 102	5762.6	5671.5(7)
Z	4	4	2	2
D _{calc} (g cm ⁻³)	1.558			1.810
F(000)	4808			3074
μ (mm ⁻¹)	1.129			2.794
λ (Å)	0.80000			0.71073
Data collected	57 445			53 918
Unique data	11 454			20 710
R _{int}	0.0330			0.0992
Parameters	553			1530
R ₁ (I > 2σ(I))	0.0778			0.0604
wR ₂ (all data)	0.2302			0.1545
S (all data)	1.029			0.969
Max. diff. peak/hole (e Å ⁻³)	+1.47/−0.93			+1.98/−3.21

the reaction kinetics and the crystallisation conditions. For example, the reaction of the *nbdea*H₂ ligand with FeCl₂, pivalic acid and Ln(NO₃)₃ yielded the hexanuclear {Fe^{III}Dy^{III}} cluster.¹³ However, an analogous cluster with the same {Fe^{III}Dy^{III}} core has been obtained by using [Fe₃O]⁷⁺ triangles coordinated by benzoic acid with Ln(NO₃)₃ and the same *nbdea*H₂ ligand.^{8a}

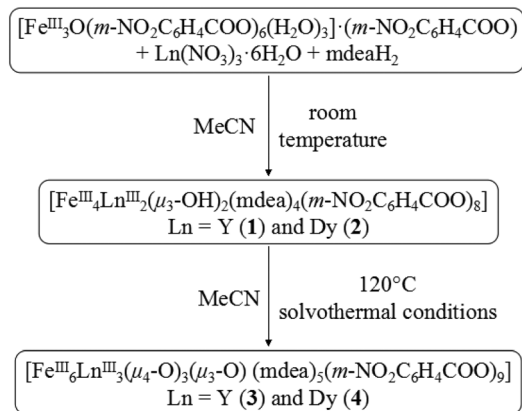
The reactions of [Fe^{III}O(*m*-NO₂C₆H₄COO)₆(H₂O)₃].(*m*-NO₂C₆H₄COO)/Ln(NO₃)₃/*mdea*H₂ in the molar ratio 1 : 1 : 8 in MeCN at room temperature afforded the hexanuclear compounds [Fe₄Ln₂(μ₃-OH)₂(*mdea*)₄(*m*-NO₂C₆H₄COO)₈].3MeCN, where Ln = Y (1) and Dy (2). Compounds [Fe₆Ln₃(μ₄-O)₃(μ₃-O)-(*mdea*)₅(*m*-NO₂C₆H₄COO)₉].3MeCN, where Ln = Y (3) and Dy (4), can be synthesised *via* a solvothermal transformation

process by heating 1 or 2 in MeCN under solvothermal conditions for 72 hours, respectively (Scheme 1).

Single-crystal X-ray analysis revealed that compound 1 crystallises in the monoclinic space group C2/c with Z = 4, while compound 4 crystallises in the triclinic space group Pī with Z = 2. Crystals of both 1 and 2 are small and weakly-diffracting, but it was possible to determine the structure of 1 using synchrotron radiation. Compounds 2 and 3 were shown to be isomorphous with 1 and 4, respectively, by comparison of their unit cells with those of compounds 1 and 4. Therefore, the structures for 1 and 4 are described here in detail as representative examples.

Compound 1 exhibits the identical {Fe₄Y₂} core unit to that previously reported for [Fe₄Ln₂(μ₃-OH)₂(*nbdea*)₄((CH₃)₃-CCO₂)₆(N₃)₂]¹³ and for [Fe₄Dy₂(μ₃-OH)₂(*nbdea*)₄(C₆H₅CO₂)₈].MeCN.^{8a} In the hexanuclear core of compound 1 there is a butterfly shaped central {Fe₂Y₂} unit, in which the FeY₂ triangles are each bridged by a single (μ₃-OH)⁻ ligand (O1 or O1'), a *syn*, *syn*-bridging benzoate and a doubly-deprotonated (*mdea*)²⁻ ligand, with the two deprotonated oxygens (O4, O5 or O4', O5') forming alkoxo bridges along the Fe...Y edges. The remaining Fe^{III} ions are linked to the tetranuclear core through two deprotonated oxygens (O2, O3 or O2', O3') from a doubly-deprotonated (*mdea*)²⁻ ligand and a *syn*, *syn*-bridging benzoate, respectively (Fig. 1).

The molecular structure of compound 4 consists of a core of six Fe^{III} and three Dy^{III} ions (Fig. 2). One of the μ₄-O²⁻ ligands, O1, bridges between Fe1 and three Dy^{III} ions (Dy1, Dy2 and Dy3) to give a distorted tetrahedral {FeDy₃(μ₄-O)} unit. The Fe1 and Dy1 are further linked through two *syn*, *syn*-bridging benzoates, while Dy2 and Dy3 are each chelated by a



Scheme 1 A schematic representation of the synthetic routes of compounds 1–4. Details are given in the Experimental section.



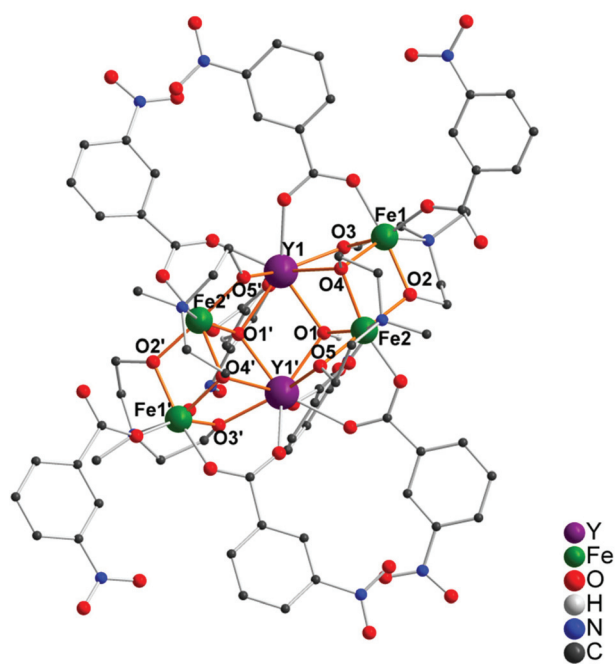


Fig. 1 Molecular structure of the coordination cluster in $[\text{Fe}_4^{\text{II}}\text{Y}_2^{\text{III}}(\mu_3\text{-OH})_2(\text{mdea})_4(\text{m-NO}_2\text{C}_6\text{H}_4\text{COO})_8]\cdot 3\text{MeCN}$ (**1**). Organic H atoms have been omitted for clarity.

benzoate ligand. The Fe1–O1 distance is 1.8714(1) Å, while the Dy–O1 bond lengths are in the range 2.2691(2)–2.3810(2) Å. The angles between Fe1 and the three Dy ions are 122.265(6)° for Fe1–O1–Dy1, 104.032(7)° for Fe1–O1–Dy2 and 103.445(7)° for Fe1–O1–Dy3, respectively, while the Dy–O1–Dy angles vary from 107.105(5)° to 110.147(4)°.

The Dy2...Dy3 edge is further bridged by a benzoate oxygen (O15) while the Dy1...Dy3 and Dy1...Dy2 edges are each

further bridged by other $\mu_4\text{-O}^{2-}$ ligands with two further Fe centres: O2 bridges Dy1, Dy3, Fe2 and Fe3, and O3 bridges Dy1, Dy2, Fe2 and Fe4. Two peripheral benzoate ligands provide two *syn,syn*-bridges between Fe3 and Dy3 or Fe4 and Dy2, respectively. The only $\mu_3\text{-O}^{2-}$ ligand O4 bridges the central Fe2 to the final two Fe^{III} ions (Fe5 and Fe6). Additionally, two further benzoate ligands form two *syn,syn*-bridges between Fe5 and Fe6. The remaining ten (mdea)²⁻ oxygens each form a (μ -OR) bridge between the iron and a further metal centre, thus forming four Fe...Fe and six Fe...Dy bridges.

In contrast to the previously reported isostructural Fe_4Ln_2 clusters with benzoate^{8a} or *t*-butylbenzoate¹³ ligands, the nitrobenzoate ligands in **1** offer additional possibilities for inter- and intermolecular interactions. Thus the molecular structure is now further stabilised by intramolecular C–H...ONO hydrogen bonds and electrostatic interactions between nitro N and O atoms of adjacent nitrobenzoate ligands. The overall crystal packing is also stabilised by a range of intermolecular C–H...ONO hydrogen bonds involving C–H bonds from either nitrobenzoate or diethanolamine ligands. Similar interactions are found in the structure of **4**.

Magnetic properties

The temperature dependence of the dc magnetic susceptibility data for compounds **1**–**4** were collected in the 1.8–300 K temperature range under a field of 1000 Oe. For the set of compounds **1** and **2**, the dc data summarised in Table S1† show that the experimental χT product at 300 K is lower than the expected value for four Fe^{III} ($S = 5/2$, $g = 2$) and two Ln^{III} non-interacting ions. For compound **1** containing diamagnetic Y^{III} ions, on lowering the temperature the χT product continuously decreases until 1.8 K, suggesting the presence of antiferromagnetic interactions between the Fe^{III} ions (Fig. 3). The experimental data of **1** were fitted to the expression for the

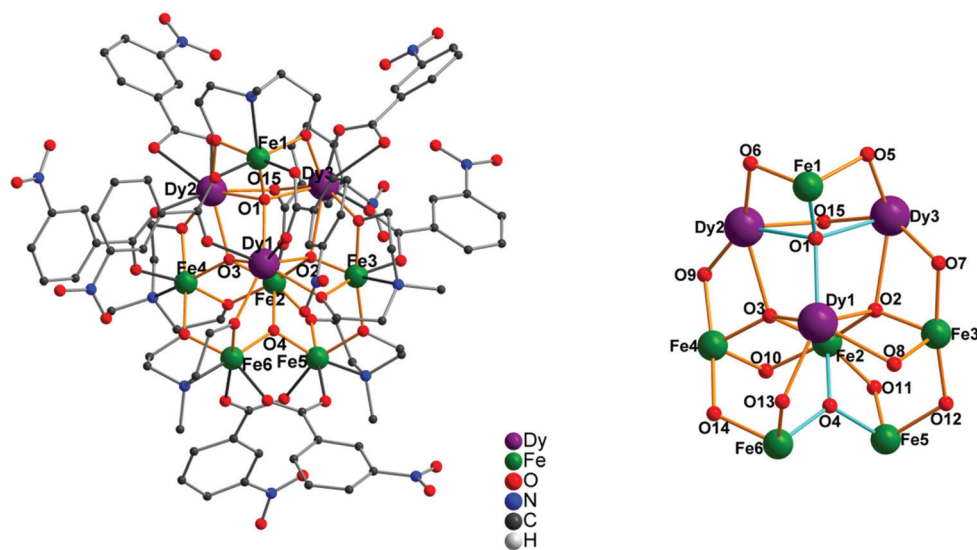


Fig. 2 Molecular structure (left) and core (right) of the coordination cluster in $[\text{Fe}_6\text{Dy}_3(\mu_4\text{-O})_3(\mu_3\text{-O})(\text{mdea})_5(\text{m-NO}_2\text{C}_6\text{H}_4\text{COO})_9]\cdot 3\text{MeCN}$ (**4**). Organic H atoms have been omitted for clarity.



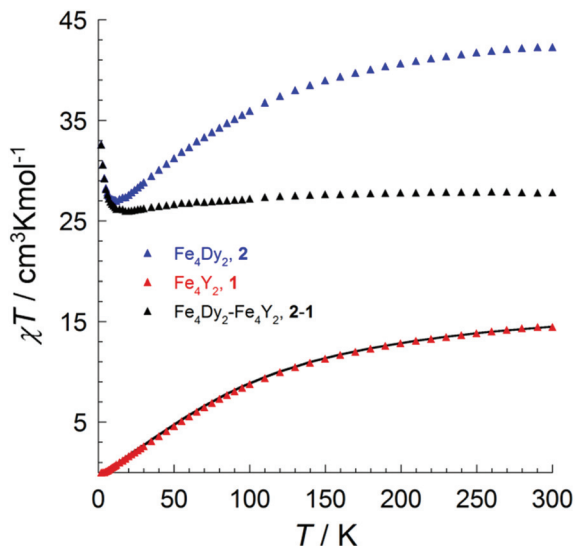


Fig. 3 Temperature dependence of the χT product at 1000 Oe for 1 (red) and 2 (blue), and the adjusted χT vs. T plot for compound 2 with the data of compound 1 subtracted (black). The solid line is the best fit to the experimental data.

molar susceptibility derived from the Hamiltonian $H = -2J \cdot S_1 \cdot S_2$. The best fit to the χT vs. T plot gave $g = 2.03$ and the exchange parameter $J = -7.04 \text{ cm}^{-1}$. This value is close to those obtained in the reported similar Fe_4Y_2 compound.¹³ The J value can also be estimated from using the magnetostructural correlations for dimers using the Fe–O lengths and Fe–O–Fe angles,¹⁴ leading to a value of $J = -10.3 \text{ cm}^{-1}$. These weak antiferromagnetic interactions between Fe^{III} ions result in a discrepancy between the experimental and calculated χT products for 1.

For compound 2, the χT product decreases on lowering the temperature, reaching a minimum value at 12 K, and then slightly increases until $32.6 \text{ cm}^3 \text{ K mol}^{-1}$ at 1.8 K, which may

result from the weak intramolecular ferromagnetic interactions within the complex (Fig. 3). Since the magnetic behaviour of 1 suggests that the $\text{Fe}^{\text{III}}-\text{Fe}^{\text{III}}$ interactions are antiferromagnetic, a subtraction of the χT product of 1 from 2 was performed to estimate the magnetic interactions related to the Dy^{III} ions (Fig. 3). The shape of the adjusted χT vs. T plot revealed that the interaction between the two central Dy^{III} ions should be weakly ferromagnetic.

The field dependence of magnetization for 1 at 2 K confirmed the presence of the dominant antiferromagnetic interactions between the Fe^{III} ions, in which the magnetization only reaches $0.05\mu_{\text{B}}$ even up to 70 kOe (Fig. S1,† top-left). For 2, the magnetization increases with increasing field at low temperature (2 K, 3 K and 5 K), reaching about $12\mu_{\text{B}}$ without saturation even at 70 kOe (Fig. S1,† top-right). The lack of saturation indicates the presence of magnetic anisotropy and/or low-lying excited states in this system. Since compound 2 contains two antiferromagnetically coupled Fe_2 units for which the magnetization at low temperature is close to zero, the value of $12\mu_{\text{B}}$ at 70 kOe is contributed by the weak ferromagnetically coupled Dy_2 unit, in which the value for the single Dy^{III} ion in polycrystalline compounds is expected to be $\sim 5-6\mu_{\text{B}}$.

For 3 and 4, the χT value at 300 K is much lower than the expected value for six high-spin Fe^{III} ($S = 5/2$, $g = 2$) and three Dy^{III} non-interacting ions (see Table S1†), respectively, which indicates strong antiferromagnetic interactions within the complexes. Upon cooling, χT values for both compounds continuously decrease until 1.8 K, confirming the dominant antiferromagnetic interactions within both complexes (Fig. 4, left). For compound 3 containing diamagnetic Y^{III} ions, the χT value of $0.75 \text{ cm}^3 \text{ K mol}^{-1}$ at 1.8 K revealed that at low temperature the interactions within the five bottom Fe^{III} ions as well as the interaction between the Fe^{III} pentamer and the single Fe^{III} ion (Fe1) are antiferromagnetic. The shape of the adjusted χT vs. T plot for compound 4 with the data of compound 3 subtracted suggested that the interactions between the three central Dy^{III}

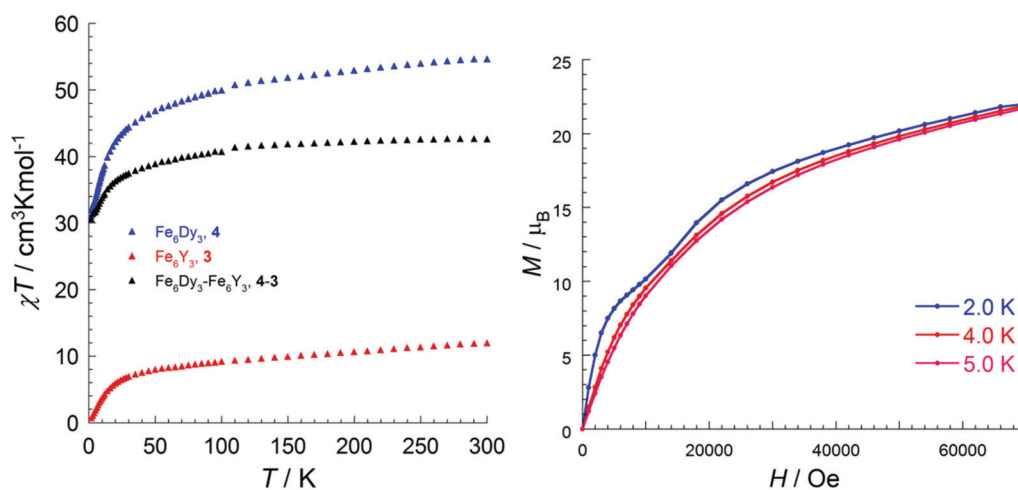


Fig. 4 (left) Temperature dependence of the χT product at 1000 Oe for 3 (red) and 4 (blue), and the adjusted χT vs. T plot for compound 4 with the data of compound 3 subtracted (black). (right) Field dependence of magnetization at low temperature for compound 4.



ions should also be antiferromagnetic (Fig. 4, left). Furthermore, the discrepancy between the χT values for 3 and 4 at 300 K is $42.7 \text{ cm}^3 \text{ K mol}^{-1}$. This value is in good agreement with the expected value ($42.5 \text{ cm}^3 \text{ K mol}^{-1}$) for three non-interacting Dy^{III} ions.

The field dependence of the magnetization at low temperature for 3 increases steadily and reaches $6.6\mu_{\text{B}}$ at 2 K and 70 Oe (Fig. S1,† bottom). This value is much lower than the expected saturation value of $10\mu_{\text{B}}$ for the parallel alignment of the single Fe^{III} ion (Fe1) ($S = 5/2$) spin and the resulting spin state of the five antiferromagnetically coupled iron ions in the Fe^{III} pentamer ($S = 5/2$). This shows that in spite of the absence of direct exchange pathways between these spin sources, they still experience each other and this results in weak antiferromagnetic interaction, leading to a lower magnetic moment of $6.6\mu_{\text{B}}$ than the expected $10\mu_{\text{B}}$.

The M vs. H data for compound 4 show that the magnetization increases with an increase in applied field in two steps at 2 K (Fig. 4, right). First, the magnetization increases sharply, reaching a step at about $10.1\mu_{\text{B}}$ at a field of 10 kOe. With a further increase in applied field, the magnetization increases rapidly again and approaches a value of $22.0\mu_{\text{B}}$ at 70 kOe. Such a behaviour indicates the stepwise alignment of spins under the applied field and the progressive population of the low-lying excited states. The value $22.0\mu_{\text{B}}$ is in good agreement with the value expected for three Dy ions in polycrystalline compounds ($\sim 15\mu_{\text{B}}$) and $6.6\mu_{\text{B}}$ from the ($\text{Fe}_5 + \text{Fe}$) unit. The lack of saturation indicates the presence of magnetic anisotropy and/or the low-lying excited states in this system.

The orientation of the main magnetic axes for all three Dy^{III} centers in 4 can be determined by using the program Magellan.¹⁵ Fig. 5 shows that the axes for Dy2 and Dy3 point towards the Dy1 while the axis for Dy1 points to the center of the Dy_3 triangle. Such an orientation leads to an incomplete cancellation of magnetic spins, resulting in a magnetic ground state for the Dy_3 triangle. The type of inflection observed at about 10 kOe is usually observed when the applied magnetic

field overwhelms weak antiferromagnetic interactions and dictates the orientation of these spins. However, the presence of very anisotropic Dy ions in this compound makes it difficult to determine the magnitude of the magnetic exchange interaction and to determine which magnetic spins are involved in this. Another factor here is that the Dy_3 triangle in 4 does not necessarily have a nonmagnetic ground state, although the structural details suggest this given our previous results on triangles with very similar structural features. Thus, although at small fields (0–10 kOe) its magnetization shows a similar behaviour to that seen for the prototype Dy_3 ,¹⁶ the non-magnetic state can be excluded since the χT of 4 at 1.8 K is far from zero (see Fig. 4, left), indicating a magnetic ground state for the Dy_3 triangle. We would need more information concerning the relative magnitudes of the exchange between Dy–Dy and Dy–Fe ions to elucidate the origin of the observed inflection.

Due to the magnetic anisotropy present in both sets of compounds, ac susceptibility measurements were performed under zero dc fields. There is no out-of-phase signal shown above 1.8 K for compounds 1 and 3. However, in the case of compound 2, both temperature- and frequency-dependent in-phase, χ' , and out-of-phase, χ'' , signals are detected, indicating slow relaxation of its magnetisation. The temperature-dependent χ'' signals showed no maximum, but some shoulders were observed, indicating the presence of quantum tunnelling effects with more than one relaxation process involved in this system (Fig. S2†). However, clear maxima were observed in the frequency-dependent χ'' signals (Fig. 6) and the Cole–Cole plots (Fig. S3†) can be fitted to a generalised Debye function resulting in $\alpha = 0.05$ – 0.16 , demonstrating that there is only one relaxation process in this system. Fitting the frequency-dependent ac susceptibility data of 2 with an Arrhenius law leads to the characteristic SMM energy barrier, U_{eff} , of 7.1 K and the relaxation time, τ_0 , of 6.4×10^{-6} s (Fig. S4†).

In order to further study this system and check for any quantum tunnelling effect above 1.8 K, the frequency dependence of the ac susceptibility was measured under different

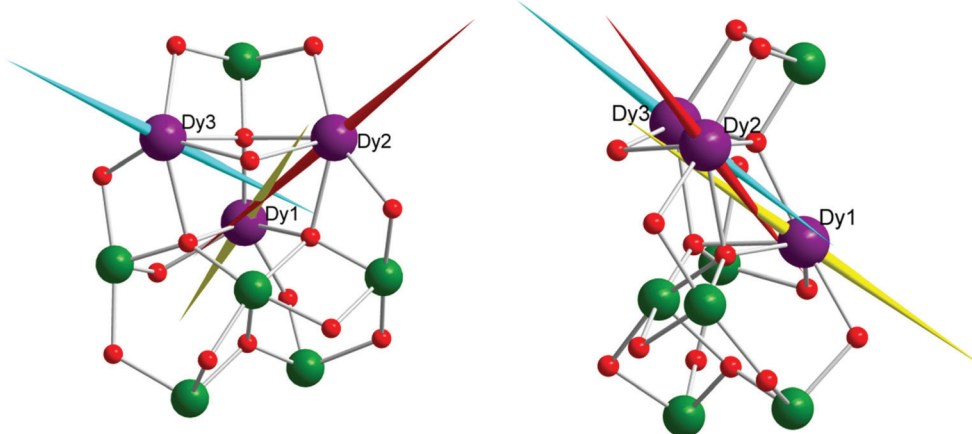


Fig. 5 Orientation of the anisotropy axes as determined using the Magellan¹⁵ program for the Dy^{III} centres (Dy1, Dy2 and Dy3) in 4.



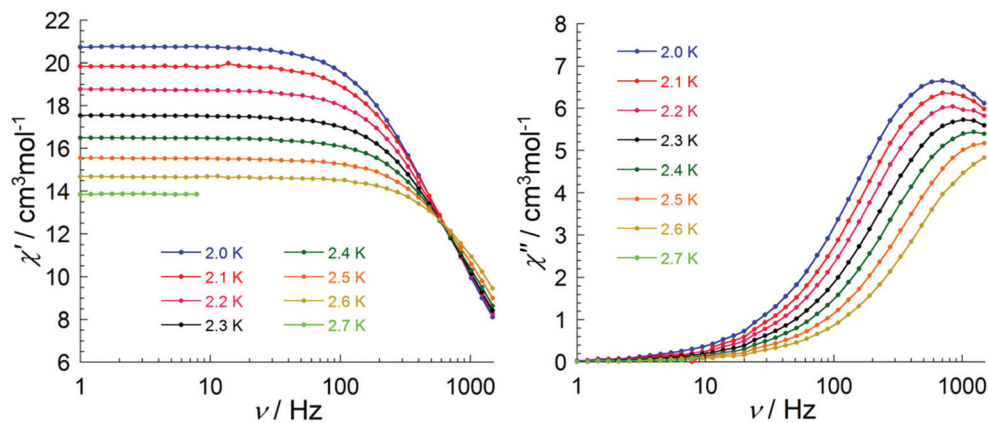


Fig. 6 Frequency dependence of the in-phase (χ') (left) and out-of-phase (χ'') (right) ac susceptibility components at the indicated temperatures in zero dc field for **2**.

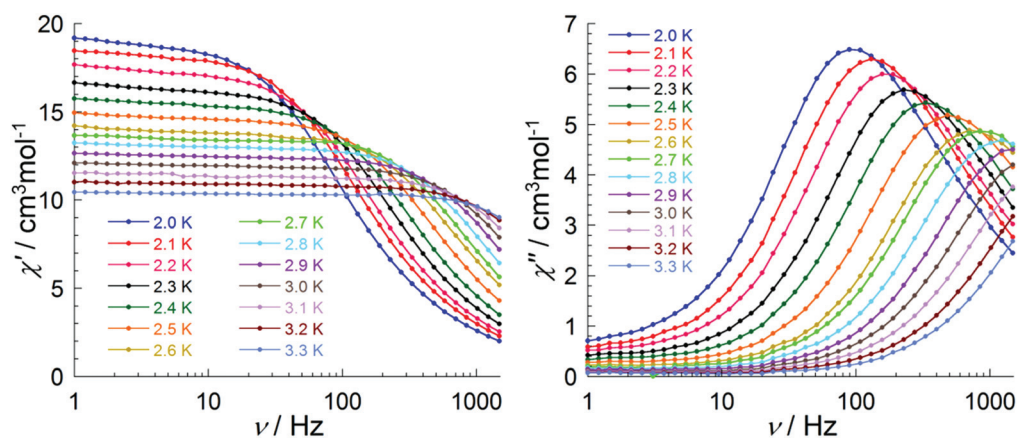


Fig. 7 Frequency dependence of the in-phase (χ') (left) and out-of-phase (χ'') (right) ac susceptibility components at the indicated temperatures under 500 Oe dc field for **2**.

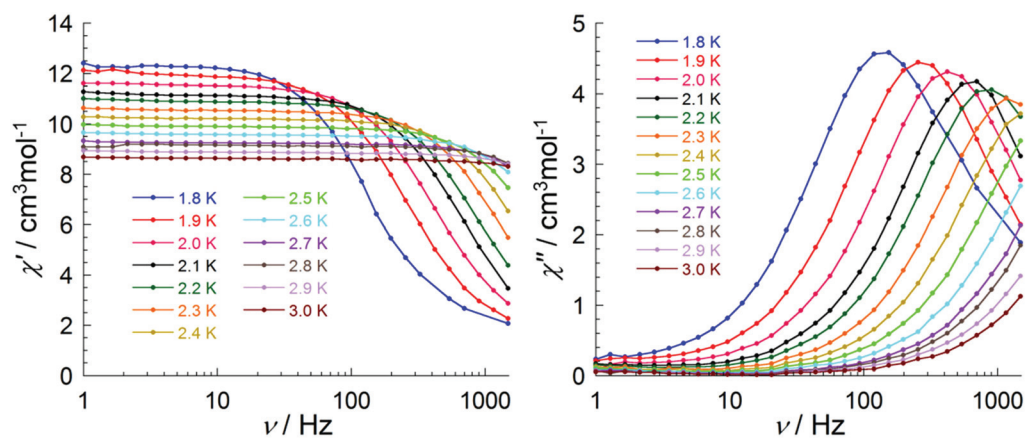


Fig. 8 Frequency dependence of the in-phase (χ') (left) and out-of-phase (χ'') (right) ac susceptibility components at the indicated temperatures under 1000 Oe dc field for **4**.



applied dc fields at 1.8 K. As shown in Fig. S5,† the maximum value in the frequency dependent out-of-phase plot increases from 110 Hz at 500 Oe to a value of 884 Hz at 2000 Oe and then slightly decreases. This observation suggests that the magnetic relaxation can be slowed down by the application of the external dc fields. Thus, ac data were collected with an applied dc field of 500 Oe and clear maxima were detected on both χ'' vs. T (Fig. S6†) and χ'' vs. ν (Fig. 7) data. The characteristic relaxation times (τ) were determined from the frequency dependence of the out-of-phase susceptibility. Fitting the data by an Arrhenius law leads to an estimation of the energy gap $U_{\text{eff}} = 18.4$ K and the relaxation time $\tau_0 = 2.0 \times 10^{-7}$ s (Fig. S7†), which further confirmed that a small external dc field slowed down the relaxation time by suppressing quantum tunnelling of magnetization.

The ac susceptibility measurement for **4** in zero dc field shows very weak out-of-phase ac signals. However, under a dc field of 1000 Oe, a clear maximum is detected on the χ'' vs. ν plot (Fig. 8). Fitting the data by an Arrhenius law leads to an estimation of the energy gap $U_{\text{eff}} = 17.1$ K and the relaxation time $\tau_0 = 7.4 \times 10^{-8}$ s (Fig. S8†).

Conclusions

Four Fe^{III}–Ln^{III} complexes containing mdea²⁻ and *m*-nitrobenzoic acid ligands have been synthesised and characterised. The isomorphous compounds **1** and **2** have been prepared under ambient conditions from the mdeaH₂ ligand, an [Fe₃O]⁷⁺ benzoate triangle and lanthanide nitrates, while compounds **3** and **4** were obtained *via* a solvothermal transformation process by heating **1** or **2** in MeCN at 120 °C, respectively. The structural and magnetic properties of all four compounds have been reported. After subtracting the contribution of compounds **1** and **3** containing diamagnetic Y^{III} ions from the χT products of **2** and **4**, the shape of the adjusted χT vs. T plot indicates that the Dy^{III}–Dy^{III} interactions within **2** are weakly ferromagnetic, while those within **4** are weakly antiferromagnetic. The ac magnetic susceptibility of the Fe₄Dy₂ complex **2** shows both temperature and frequency dependence. The frequency-dependent data could be fitted to the Arrhenius law, leading to an energy gap of 7.1 K and the relaxation time of 6.4×10^{-6} s. By the application of a 500 Oe dc field, the energy gap increases to 18.4 K and the relaxation time decreases to 2.0×10^{-7} s, suggesting that the external dc field can slow down the relaxation time by suppressing quantum tunnelling of magnetization. Furthermore, compound **4** exhibits out-of-phase ac susceptibility signals, which indicates that this compound is also a SMM.

Acknowledgements

Financial support from the DFG SFB TR88 “3MET” is gratefully acknowledged.

We acknowledge the Synchrotron Light Source ANKA for provision of instruments at the SCD beamline for the structural determination of compound **1**, and we would like to thank Dr Gernot Buth for assistance in using the beamline.

Notes and references

- (a) M. Murrie, *Chem. Soc. Rev.*, 2010, **39**, 1986; (b) G. E. Kostakis, A. M. Ako and A. K. Powell, *Chem. Soc. Rev.*, 2010, **39**, 2238; (c) X.-Y. Wang, C. Avendano and K. R. Dunbar, *Chem. Soc. Rev.*, 2011, **40**, 3213.
- G. Christou, D. Gatteschi, D. N. Hendrickson and R. Sessoli, *MRS Bull.*, 2000, **25**, 66.
- (a) R. Sessoli and A. K. Powell, *Coord. Chem. Rev.*, 2009, **253**, 2328; (b) M. Andruh, J.-P. Costes, C. Diaz and S. Gao, *Inorg. Chem.*, 2009, **48**, 3342; (c) G. E. Kostakis, I. J. Hewitt, A. M. Ako, V. Mereacre and A. K. Powell, *Philos. Trans. R. Soc., A*, 2010, **368**, 1509.
- (a) J. W. Sharples and D. Collison, *Coord. Chem. Rev.*, 2014, **260**, 1; (b) K. Liu, W. Shi and P. Cheng, *Coord. Chem. Rev.*, 2015, **289**, 74.
- (a) R. W. Saalfrank, A. Scheurer, I. Bernt, F. W. Heinemann, A. V. Postnikov, V. Schünemann, A. X. Trautwein, M. S. Alam, H. Rupp and P. Müller, *Dalton Trans.*, 2006, 2865; (b) A. M. Ako, O. Waldmann, V. Mereacre, F. Klöwer, I. J. Hewitt, C. E. Anson, H. U. Güdel and A. K. Powell, *Inorg. Chem.*, 2007, **46**, 756; (c) R. W. Saalfrank, C. Deutscher, S. Sperner, T. Nakajima, A. M. Ako, E. Uller, F. Hampel and F. W. Heinemann, *Inorg. Chem.*, 2004, **43**, 4372; (d) E. M. Rumberger, L. N. Zakharov, A. L. Rheingold and D. N. Hendrickson, *Inorg. Chem.*, 2004, **43**, 6531.
- (a) L. Ungur, S. K. Langley, T. N. Hooper, B. Moubaraki, E. K. Brechin, K. S. Murray and L. F. Chibotaru, *J. Am. Chem. Soc.*, 2012, **134**, 18554; (b) S. K. Langley, B. Moubaraki and K. S. Murray, *Polyhedron*, 2013, **64**, 255; (c) S. K. Langley, B. Moubaraki and K. S. Murray, *Inorg. Chem.*, 2012, **51**, 3947.
- (a) S. K. Langley, C. M. Forsyth, B. Moubaraki and K. S. Murray, *Dalton Trans.*, 2015, **44**, 912; (b) S. Schmidt, D. Prodius, V. Mereacre, G. E. Kostakis and A. K. Powell, *Chem. Commun.*, 2013, **49**, 1696; (c) S. Schmidt, D. Prodius, G. Novitchi, V. Mereacre, G. E. Kostakis and A. K. Powell, *Chem. Commun.*, 2012, **48**, 9825; (d) S. Nayak, O. Roubeau, S. J. Teat, C. M. Beavers, P. Gamez and J. Reedijk, *Inorg. Chem.*, 2010, **49**, 216.
- (a) S. Chen, V. Mereacre, D. Prodius, G. E. Kostakis and A. K. Powell, *Inorg. Chem.*, 2015, **54**, 3218; (b) E. J. L. McInnes, C. Anson, A. K. Powell, A. J. Thomson, S. Pousserau and R. Sessoli, *Chem. Commun.*, 2001, 89.
- (a) X. Bao, W. Liu, J.-L. Liu, S. Gómez-Coca, E. Ruiz and M.-L. Tong, *Inorg. Chem.*, 2013, **52**, 1099; (b) W.-Q. Chen, Y.-M. Chen, T. Lei, W. Liu and Y. Li, *Inorg. Chem. Commun.*, 2012, **19**, 4; (c) S. Wöhlert, M. Wriedt, T. Fic, Z. Tomkowicz, W. Haase and C. Näther, *Inorg. Chem.*, 2013, **52**, 1061;



- (d) J. T. Greenfield, S. Kamali, N. Izquierdo, M. Chen and K. Kovnir, *Inorg. Chem.*, 2014, **53**, 3162.
- 10 R. F. Weinland and A. Herz, *Ber. Dtsch. Chem. Ges.*, 1912, **45**, 2662.
- 11 G. M. Sheldrick, *Acta Crystallogr., Sect. A: Fundam. Crystallogr.*, 2008, **64**, 112.
- 12 (a) Y.-F. Zeng, G.-C. Xu, X. Hu, Z. Chen, X.-H. Bu, S. Gao and E. C. Sañudo, *Inorg. Chem.*, 2010, **49**, 9734; (b) A. Baniodeh, I. J. Hewitt, V. Mereacre, Y. Lan, G. Novitchi, C. E. Anson and A. K. Powell, *Dalton Trans.*, 2011, **40**, 4080; (c) A. Baniodeh, C. E. Anson and A. K. Powell, *Chem. Sci.*, 2013, **4**, 4354; (d) V. Mereacre, D. Prodius, Y. Lan, C. Turta, C. E. Anson and A. K. Powell, *Chem. – Eur. J.*, 2011, **17**, 123; (e) A. M. Ako, V. Mereacre, R. Clérac, I. J. Hewitt, Y. Lan, C. E. Anson and A. K. Powell, *Dalton Trans.*, 2007, 5245; (f) A. Baniodeh, V. Mereacre, N. Magnani, Y. Lan, J. A. Wolny, V. Schünemann, C. E. Anson and A. K. Powell, *Chem. Commun.*, 2013, **49**, 9666.
- 13 V. Mereacre, F. Klöwer, Y. Lan, R. Clérac, J. A. Wolny, V. Schünemann, C. E. Anson and A. K. Powell, *Beilstein J. Nanotechnol.*, 2013, **4**, 807.
- 14 (a) S. M. Gorun and S. J. Lippard, *Inorg. Chem.*, 1991, **30**, 1625; (b) H. Weihe and H. U. Güdel, *J. Am. Chem. Soc.*, 1997, **119**, 6539; (c) C. Canàda-Vilalta, T. A. O'Brien, E. K. Brechin, M. Pink, E. R. Davidson and G. Christou, *Inorg. Chem.*, 2004, **43**, 5505; (d) S. Mukherjee, R. Bagai, K. A. Abboud and G. Christou, *Inorg. Chem.*, 2011, **50**, 3849.
- 15 N. F. Chilton, D. Collison, E. J. L. McInnes, R. E. P. Winpenny and A. Soncini, *Nat. Commun.*, 2013, **4**, 2551.
- 16 J. Tang, I. Hewitt, N. T. Madhu, G. Chastanet, W. Wernsdorfer, C. E. Anson, C. Benelli, R. Sessoli and A. K. Powell, *Angew. Chem., Int. Ed.*, 2006, **45**, 1729.

